Geochemistry Geophysics Geosystems G3
AN ELECTRONIC JOURNAL OF THE EARTH SCIENCES
Published by AGU and the Geochemical Society

Article
Volume 5, Number 4
20 April 2004
Q04007, doi:10.1029/2003GC000639
ISSN: 1525-2027

Evidence for the submarine weathering of silicate minerals in Black Sea sediments: Possible implications for the marine Li and B cycles

G. Aloisi, K. Wallmann, and M. Drews
GEOMAR-Research Centre for Marine Geosciences, Wischhofstrasse 1–3, D-24148 Kiel, Germany (valoisi@geomar.de)

G. Bohrmann
Department of Geosciences, University of Bremen, Klagenfurter Strasse, D-28359 Bremen, Germany

[1] The role of sediment diagenesis in the marine cycles of Li and B is poorly understood. Because Li and B are easily mobilized during burial and are consumed in authigenic clay mineral formation, their abundance in marine pore waters varies considerably. Exchange with the overlying ocean through diffusive fluxes should thus be common. Nevertheless, only a minor Li sink associated with the low-temperature alteration of volcanic ash has been observed. We describe a low-temperature diagenetic environment in the Black Sea dominated by the alteration of detrital plagioclase feldspars. Fluids expelled from the Odessa mud volcano in the Sorokin Trough originate from shallow (≈100–400 m deep) sediments which are poor in volcanic materials but rich in anorthite. These fluids are depleted in Na^+, K^+, Li^+, B, and ^{18}O and enriched in Ca^{2+} and Sr^{2+}, indicating that anorthite is dissolving and authigenic clays are forming. Using a simple chemical model, we calculate the pH and the partial pressure of CO_2 (P_{CO2}) in fluids associated with this alteration process. Our results show that the pH of these fluids is up to 1.5 pH units lower than in most deep marine sediments and that P_{CO2} levels are up to several hundred times higher than in the atmosphere. These conditions are similar to those which favor the weathering of silicate minerals in subaerial soil environments. We propose that in Black Sea sediments enhanced organic matter preservation favors CO_2 production through methanogenesis and results in a low pore water pH, compared to most deep sea sediments. As a result, silicate mineral weathering, which is a sluggish process in most marine diagenetic environments, proceeds rapidly in Black Sea sediments. There is a potential for organic matter-rich continental shelf environments to host this type of diagenesis. Should such environments be widespread, this new Li and B sink could help balance the marine Li and Li isotope budgets but would imply an apparent imbalance in the B cycle.

Components: 12,262 words, 7 figures, 2 tables.

Keywords: Black Sea; diagenesis; silicates; weathering.

Index Terms: 1045 Geochemistry: Low-temperature geochemistry; 4802 Oceanography: Biological and Chemical: Anoxic environments; 4885 Oceanography: Biological and Chemical: Weathering.

Received 23 September 2003; **Revised** 30 January 2004; **Accepted** 2 February 2004; **Published** 20 April 2004.

Aloisi, G., K. Wallmann, M. Drews, and G. Bohrmann (2004), Evidence for the submarine weathering of silicate minerals in Black Sea sediments: Possible implications for the marine Li and B cycles, *Geochem. Geophys. Geosyst.*, *5*, Q04007, doi:10.1029/2003GC000639.

1. Introduction

[2] The marine geochemical cycles of Li and B are relevant to diverse geological topics such as the reconstruction of seawater pH evolution, mid-ocean ridge hydrothermalism and the alteration of oceanic crust [*Chan et al.*, 1992, 1993; *Smith et al.*, 1995; *Lemarchand et al.*, 2002]. It is important to constrain the modern marine Li and B budgets if Li and B geochemistry is to be used to understand present and past geological processes [e.g., *Lemarchand et al.*, 2002]. Whereas significant progress has been made in estimating the riverine and hydrothermal sources [*Stoffyn-Egli and Mackenzie*, 1984; *Spivack and Edmond*, 1987; *Huh et al.*, 1998; *Lemarchand et al.*, 2002] and the water column and low-temperature basalt alteration sinks [*Seyfried et al.*, 1984; *Chan et al.*, 1992; *Zhang et al.*, 1998], knowledge of the role played by sediments in the marine Li and B cycles is still limited.

[3] The good correlation between Li and B abundance in marine sediments indicates that these elements have a similar geochemical behavior [*You et al.*, 1995]. In the water column, Li and B adsorb to the surface of clay minerals [*Spivack et al.*, 1987; *Zhang et al.*, 1998]. After deposition and during burial, Li and B are released to pore fluids through desorption [*Zhang et al.*, 1998; *Deyhle and Kopf*, 2002]. Li and B are further released during progressive burial (starting from T $\approx$ 50–60°C) from pelagic sediments [*Chan et al.*, 1994; *You et al.*, 1996; *Zhang et al.*, 1998], following clay mineral dehydration/transformation processes [*Ishikawa and Nakamura*, 1993; *Chan and Kastner*, 2000] and during high-temperature reactions in the underlying oceanic or continental crust [*Stoffyn-Egli and Mackenzie*, 1984; *Martin et al.*, 1991]. Expulsion of Li- and B-rich pore fluids at convergent margins and sediment-ocean diffusive fluxes of Li produced by high-temperature seawater-basalt interaction have been tentatively quantified [*You et al.*, 1995; *Zhang et al.*, 1998]. Compared to diagenetic sources of Li and B, diagenetic sinks seem to be less common. The low-temperature alteration of volcanic ash to clay minerals [*McDuff and Gieskes*, 1976; *Egeberg et al.*, 1990] concentrates Li in the authigenic clay, so that pore waters become Li-poor [*Martin et al.*, 1991; *Spivack et al.*, 1987; *Zhang et al.*, 1998]. A similar behavior is expected for B, since B is consumed during low-temperature alteration of basaltic rocks [*Spivack et al.*, 1987]. Thus portions of the seafloor underlain by volcanic ashes undergoing diagenesis may act as Li, and likely B, sinks [*Zhang et al.*, 1998].

[4] The role of detrital silicate mineral diagenesis in the marine Li and B cycles has not yet been investigated. In the subaerial weathering process, Li is released from primary silicate minerals and is concentrated in authigenic clays, so that the remaining fluid is Li-poor [*Morozov*, 1969; *Ronov et al.*, 1970; *Anderson et al.*, 1989]. Thus, if alteration of primary silicate minerals takes place in marine sediments, it could represent a previously unaccounted Li sink. The dissolution of silicate minerals is favored at low pH. In the subaerial environment, pedogenetic processes lower the pH of pore fluids considerably, such that the rates of silicate mineral dissolution are high [*Stumm and Morgan*, 1996]. In most marine pore waters, however, the pH is relatively stable due to buffering ($\approx$7.2–7.6), such that the dissolution of silicate minerals proceeds very slowly. Thus, although primary silicate minerals such as feldspars and micas are common detrital constituents of most marine sediments, they undergo a comparatively less intense diagenesis than volcanic ashes or basaltic rocks [*Kastner*, 1981].

[5] During DSDP Leg 42A in the Black Sea, a shallow ($\approx$100–400 m) sediment interval undergoing intense silicate alteration processes was drilled in the central abyssal plain at Site 379 [*Manheim and Schug*, 1978] (Figure 1). In the pore waters of these sediments, Ca^{2+} is produced and K^+ and Na^+ are consumed by diagenetic processes. *Manheim and Schug* [1978] pointed out that this trend is consistent with low-temperature volcanic ash alteration processes. However, analysis of the lithology and mineralogy of sediments obtained during DSDP Leg 42A showed that volcanic ashes or basaltic rocks are very scarce in Black Sea sediments and are absent at site 379 [*Shimkus et al.*, 1978; *Trimonis et al.*, 1978]. Instead, Black Sea sediments are rich in detrital silicate minerals such as quartz and feldspars [*Stoffers and Müller*, 1978].

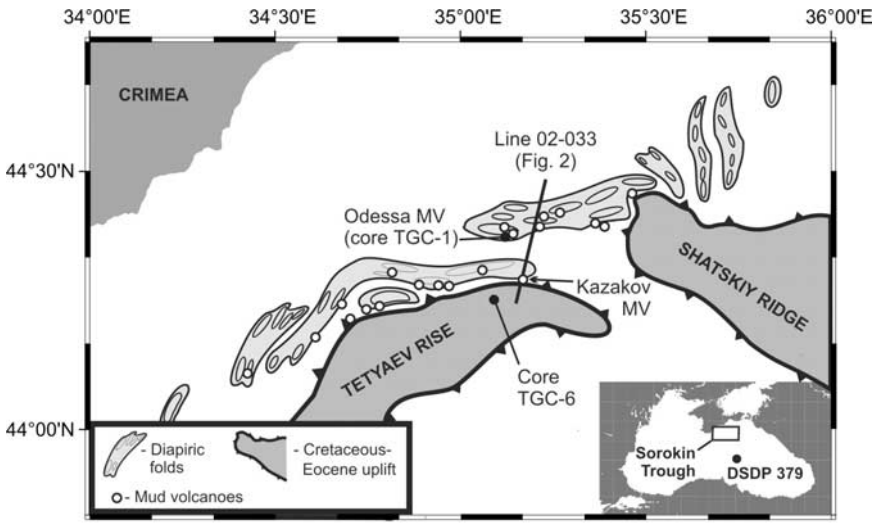

Figure 1. Location map showing the areas of mud diapirism and mud volcanism in the Sorokin Trough (redrawn after *Woodside et al.* [1997] and *Krastel et al.* [2004]). The position of the Odessa mud volcano and of seismic line 02-033 are indicated.

Our goal is to understand the role played by these silicates in the diagenetic process described by *Manheim and Schug* [1978] with particular attention to the behavior of Li and B. We carried out a geochemical study of fluids expelled from the Odessa mud volcano in the Sorokin Trough which we argue originate from the shallow sediment interval undergoing silicate digenesis. We have significantly expanded the geochemical data set of *Manheim and Schug* [1978] in order to fully characterize this diagenetic environment. To investigate the possibility that detrital silicates are undergoing dissolution, we apply a simple chemical model to calculate the pH and P_{CO2} of anoxic Black Sea pore waters. The finding that conditions favoring silicate mineral dissolution (low pH and elevated P_{CO2}) are met in Black Sea sediments is followed by a discussion of the potential impact of submarine silicate weathering on the marine Li and B cycles.

2. Studied Sites

[6] The Odessa mud volcano is part of a mud volcano field located in the Sorokin Trough, on the south-eastern margin of the Crimean Peninsula (Figure 1). In this area, most mud volcanoes develop above mud diapirs [*Bohrmann et al.*, 2004; *Krastel et al.*, 2004]. The driving force for mud diapirism is thought to be the N-S compressive regime generated by the northward motion of the buried Tetyaev and Shatskii rises (Figure 1). These structural highs act as rigid buttresses against which clays of the Maikopian formation (Oligocene – Lower Miocene) are deformed, acquire their overpressured character and rise diapirically [*Woodside et al.*, 1997].

[7] The Odessa mud volcano lies on the culmination of a WSW-ENE trending mud diapiric ridge (Figure 1). On seismic section 02–003, remobilized mud of diapiric and volcanic origin is acoustically transparent (Figure 2). The diapiric character of the mud intrusion underlying the Odessa mud volcano is evident on the basis of the upward bending of the surrounding sedimentary sequence. Core TGC-1 (44°23.01′N, 35°09.28′E, 1836 m water depth) was taken on the eastern flank of the mud volcano, roughly 1.5 km from the volcano center, during R/V METEOR cruise 52-1 [*Bohrmann and Schenck*, 2002]. It contains 410 cm of gray to dark gray hemipelagic mud which gives off a strong smell of H_2S in its shallowest part (Figure 3). A 2 cm thick carbonate crust is located at 23 cm depth in correspondence of a very sharp color boundary

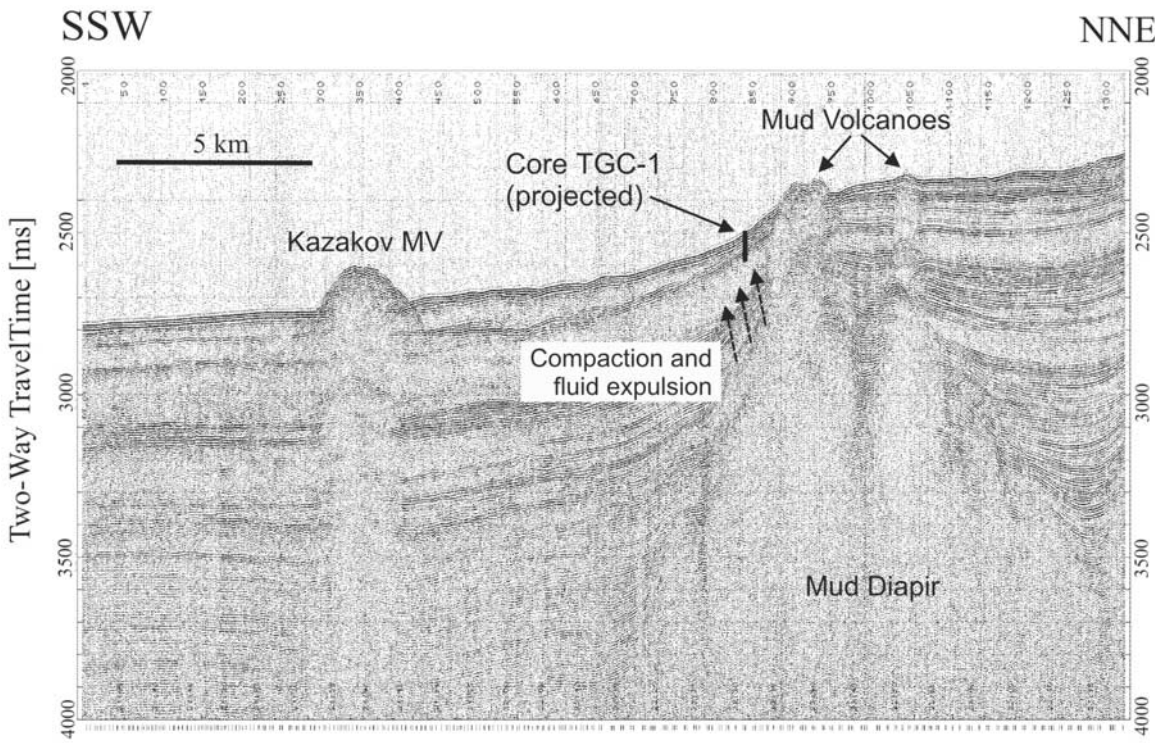

Figure 2. Seismic line 02-033 located in the vicinity of the Odessa mud volcano [from *Krastel et al.*, 2004]. The projected position of core TGC-1 is marked on the profile.

separating dark gray mud, above the crust, from a black sapropel layer below it. A second sapropel layer is present between 81 and 83 cm. Millimeter-sized gas hydrate crystals are dispersed in the mud between 123 and 140 cm and occur in lenses between 260 and 310 cm. Both the smell of H_2S and the presence of gas hydrates indicate that these sediments are influenced by the seepage of CH_4-rich fluids. Core TGC-6 (44°14.03′N, 34°58.85′E, 2161 m water depth) was taken 10 nautical miles south-west of the Odessa mud volcano on the northern slope of the Sorokin Trough. It consists of 310 cm of dark gray, homogeneous hemipeagic mud with several layers rich in bivalve shell debris. This core is used as a reference core to investigate the pore water chemistry of sediments unaffected by the seepage of methane-rich fluids in the Sorokin Trough.

3. Sampling and Chemical Analysis

[8] Coring was carried out with a 6 m long gravity corer [*Bohrmann and Schenck*, 2002]. After recovery, sediment cores were split on deck and rapidly sub-sampled. Pore water extraction by squeezing was carried out in the on-board laboratory which was cooled at 4°C to prevent heating. Pore waters were analyzed on board for dissolved ammonia ($NH_4 = [NH_4^+] + [NH_3]$) and sulfide ($H_2S = [H_2S] + [HS^-] + [S^{2-}]$) using standard photometric procedures. Total alkalinity (TA) was determined by titration immediately after pore water separation. The remaining pore waters were later analyzed in the shore-based laboratory for dissolved anions (SO_4^{2-}, Cl^-, I^-, Br^-) and dissolved elements (Na^+, K^+, Li^+, Mg^{2+}, Ca^{2+}, Sr^{2+}, Ba^{2+}, B ($=[B(OH)_3] + [B(OH)_4^-]$), Si($= [H_4SiO_4] + [H_3SiO_4^-]$) using ion chromatography and optical ICP, respectively. Sub-samples for dissolved Ca analysis were acidified immediately after squeezing to prevent further $CaCO_3$ precipitation. Sediment pH was measured in the 4°C laboratory with a pH electrode calibrated using a buffer prepared in artificial seawater [*Dickson*, 1993]. All analytical procedures applied on board and in our GEOMAR laboratories are documented in detail at

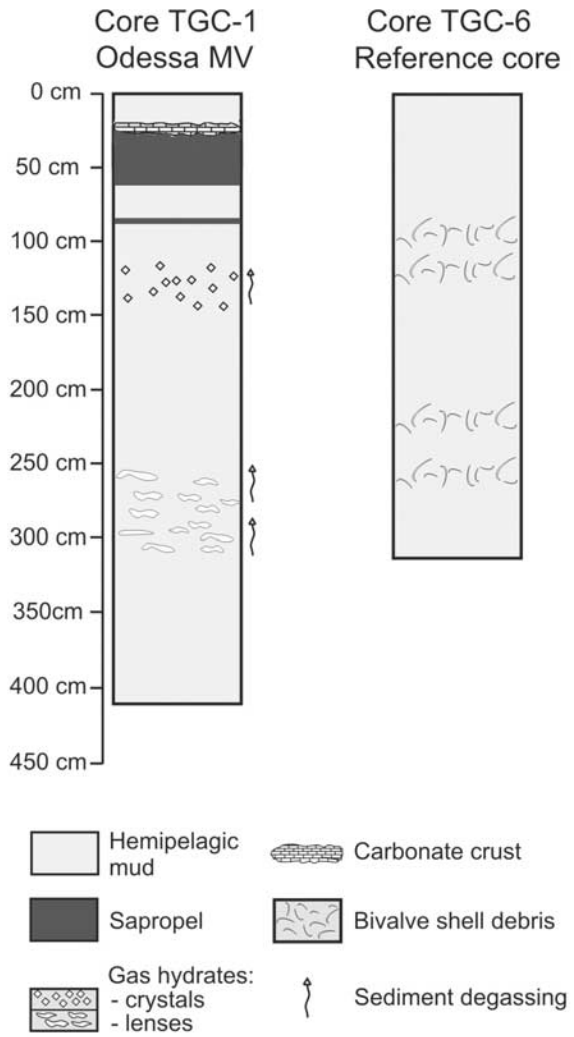

Figure 3. Lithological logs of sediment cores TGC-1 and TGC-6.

http://www.geomar.de/zd/labs/labore_umwelt/Meth_ englisch.html.

4. Results

[9] The concentration profiles of Na^+, Cl^-, Mg^{2+}, SO_4^{2-}, K^+, Si, B, Li^+, Ca^{2+}, Sr^{2+}, Ba^{2+}, NH_4, H_2S, Br^- and I^- and profiles of $\delta^{18}O_{H2O}$, TA, Br^-/Cl^- and I^-/Cl^- at sites TGC-6 and TGC-1 are shown in Figures 4 and 5, respectively. The complete chemical and isotopic data set is summarized in Table 1.

[10] At the reference site (core TGC-6), the concentration of Na^+, Cl^-, Mg^{2+}, K^+, B, Li^+ and Br^- approaches that in bottom waters (Table 2) at 2.5 cm depth and decreases downcore to various degrees. The Si concentration is higher than that of bottom waters in the top meter and then decreases downcore. The concentration of Ca^{2+}, Sr^{2+} and Ba^{2+} is equal to that in bottom waters in the top 140 cm and increases below this depth. Dissolved sulfate attains complete depletion in the top 140 cm. Total alkalinity and H_2S show concentration maxima at 172 and 42 cm depth, respectively. NH_4 and I^- increase fairly steadily downcore. The I^-/Cl^- ratio increases downcore while the Br-/Cl- ratio is nearly constant. Pore water $\delta^{18}O$ decreases downcore from values approaching those of bottom waters at the core top to −3‰ at the core base. The chemical trends at the Odessa site (core TGC-1) are similar to those at the reference site, although most concentration profiles are concave upward and gradients are mostly concentrated in the upper 100 cm of sediments. Thus the depth of complete sulfate depletion, of maximum H_2S concentration and of maximum total alkalinity all occur in the top 80 cm. In contrast to site TGC-6, the Br^- concentration increases downcore producing an increase in the Br^-/Cl^- ratio.

5. Discussion

5.1. Background Pore Water Chemistry in the Sorokin Trough (Reference Core TGC-6)

5.1.1. Influence of Buried Fresh Pore Waters

[11] Fluids at the base of core TGC-6 (Table 1) are considerably less saline than modern Black Sea bottom waters (Table 2). The concentration profiles of Na^+, Cl^-, Li^+ and K^+, which behave conservatively in the top few meters of sediments, are roughly linear indicating downward diffusion of these solutes. The small step present in the profiles at 140 cm depth is likely due to a local porosity minimum (at 140 cm the porosity is 0.6 while it is about 0.7 in the rest of the core, data not shown). Pore water chemical surveys have already shown a decrease in chlorinity with depth in the top few meters of Black Sea sediments [*Manheim and Chan*, 1974; *Jørgensen et al.*, 2001]. This feature

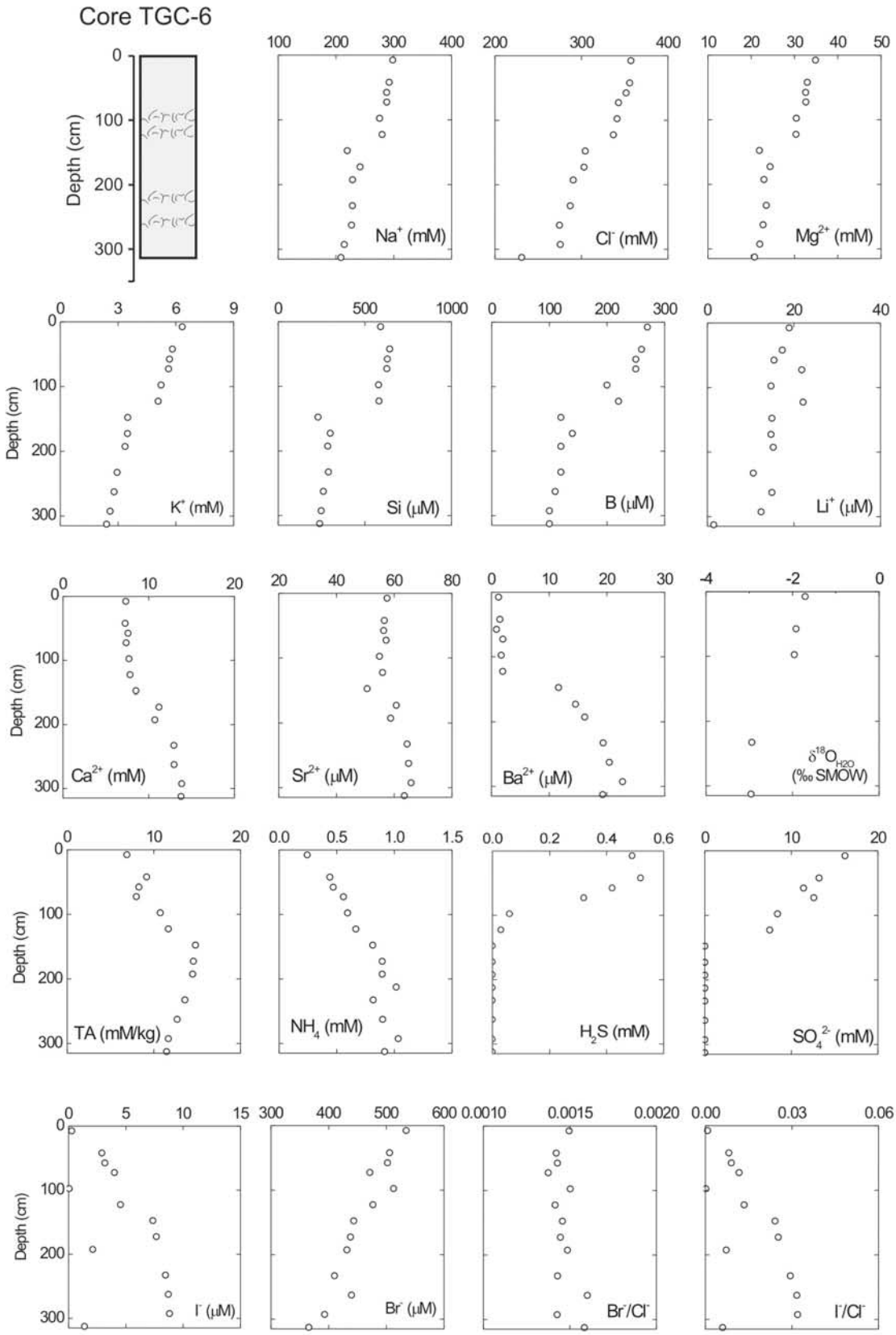

Figure 4. Measured geochemical profiles in reference core TGC-6.

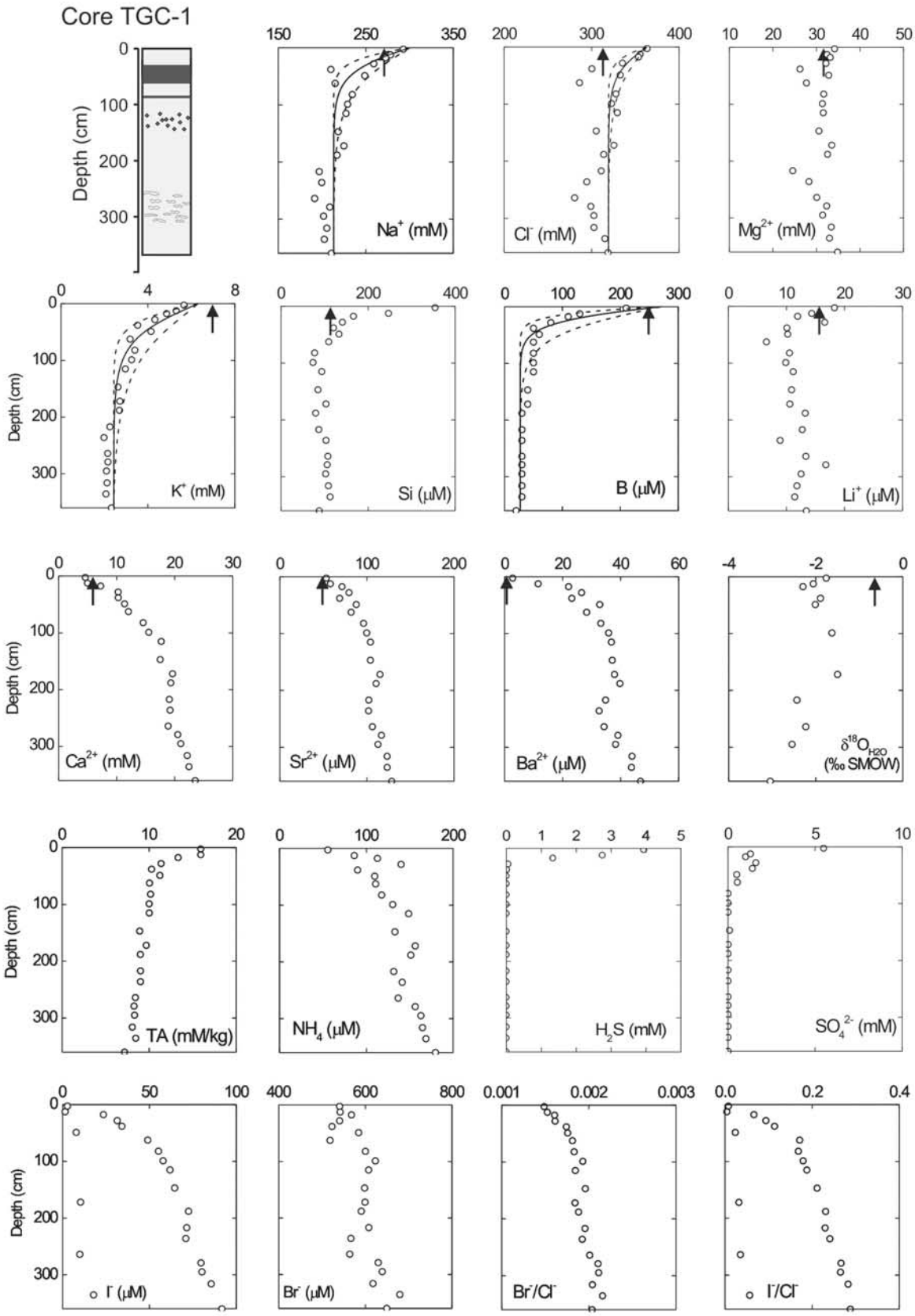
Core TGC-1
Depth (cm)
Na+ (mM)
Cl- (mM)
Mg2+ (mM)
K+ (mM)
Si (µM)
B (µM)
Li+ (µM)
Ca2+ (mM)
Sr2+ (µM)
Ba2+ (µM)
δ18OH2O (‰ SMOW)
TA (mM/kg)
NH4 (µM)
H2S (mM)
SO4 2- (mM)
I- (µM)
Br- (µM)
Br-/Cl-
I-/Cl-

Figure 5

is attributed to diffusion of Cl^- from bottom waters toward low-salinity pore fluids deposited during the Limnic period (<9000 yBP [*Boudreau and Leblond*, 1989]) when the Black Sea was a fresh water lake [*Manheim and Schug*, 1978]. Decreasing concentrations of Na^+, Cl^-, Mg^{2+}, Li^+, K^+, B, Si and Br^-, as well as decreasing pore water $\delta^{18}O$ values in core TGC-6 are consistent with the presence of fresh, ^{18}O-poor pore fluids at depth, confirming this interpretation. The very high concentration of Ca^{2+}, Sr^{2+} and Ba^{2+} at the bottom of the core indicate that simple dilution cannot account for the chemistry of buried Black Sea pore fluids. The controls on the chemistry of buried pore waters will be discussed in section 5.2.

5.1.2. Biogeochemical Processes

[12] The oxidation of organic matter using sulfate increases total alkalinity through production of HS^- and HCO_3^- and releases NH_4, Br^- and I^- [*Jørgensen*, 1982; *Martin et al.*, 1993]. In core TGC-6, the downcore increase in NH_4 and in the Br^-/Cl^- and I^-/Cl^- ratios is consistent with production of NH_4, Br^- and I^- through organic matter degradation processes. Furthermore, the depth of complete sulfate depletion corresponds to that of maximum total alkalinity, suggesting that organic matter degradation proceeds through sulfate reduction in the top 140 cm of the core. Interestingly, however, the maximum in H_2S is low (≈0.5 mM) and centered in the upper part of the core, where sulfate is still high. This could be due to loss of H_2S through a benthic flux or through precipitation of sulfides like pyrite (FeS_2) below 140 cm depth. The downcore increase in NH_4 and in the I^-/Cl^- ratio continues below 140 cm depth suggesting that organic matter degradation processes proceed through methanogenesis in the absence of sulfate [*Claypool and Kaplan*, 1974]. These observations are consistent with those of *Jørgensen et al.* [2001] who show that in Black Sea sediments beyond the shelf break sulfate reduction is the dominant organic matter degradation process in the top 2–3 m of sediments. This process accounts for 89–93% of the sulfate reduction rate, while the anaerobic oxidation of upward diffusing biogenic methane (AOM) is responsible for the remaining 7–11% [*Jørgensen et al.*, 2001]. The shape of Ca^{2+}, Ba^{2+} and Sr^{2+} concentration profiles indicates consumption of these solutes though mineral precipitation processes at 140 cm depth. Most likely, calcium is consumed through the precipitation of authigenic carbonates, fueled by AOM [*Luff and Wallmann*, 2003], while Ba and Sr are consumed through the precipitation of strontian barite, fueled by downward diffusion of sulfate and upward diffusion of Ba and Sr [*Torres et al.*, 1996; *Aloisi et al.*, 2004].

5.2. Expulsion of Chemically Altered Fluids From the Eastern Flank of the Odessa Mud Volcano

5.2.1. Seepage Rate and Source Depth

[13] At site TGC-1, convex upward profiles of most solutes suggest that upward seepage of fluids is taking place. Should this be the case, the chemistry of the expelled fluids could provide insight regarding the diagenetic processes which take place in the source area or along the fluid migration path. A simple numerical model was applied to test if seepage of fluids is taking place at site TGC-1.

[14] Assuming that Na^+, B, K^+ and Cl^- behave conservatively in the top few meters of sediments and that molecular diffusion and advection are the only transport processes affecting their concentration profiles, the steady state distribution of these solutes can described by the following second order differential equation [*Berner*, 1980]:

$$0 = \frac{\partial}{\partial x}\left(D_s(x)\cdot\phi(x)\cdot\frac{\partial C(x)}{\partial x}\right) - \phi(x)\cdot u(x)\cdot\frac{\partial C(x)}{\partial x}, \quad (1)$$

where C, in μmol cm^{-3}, is the concentration and D_s, in cm^2 a^{-1}, is the whole sediment diffusion

Figure 5. Measured and simulated geochemical profiles in core TGC-1 from the Odessa mud volcano. Measured concentrations are plotted as circles. Concentration profiles of Na^+, K^+, B and Cl^- from steady state simulations are plotted as solid and dashed lines. Solid lines represent the best fit between measured and simulated concentrations, attained using a seepage rate of 5 cm a^{-1}. Dashed lines are simulated profiles with respectively twice and half the seepage rate. Arrows represent calculated solute concentrations and the $\delta^{18}O$ of the parent pore fluid (see section 5.2.2).

Table 1. Chemical and Isotopic Composition of Pore Fluids in Cores TGC-1 and TGC-6

Core Depth, cm	Na, mM	Cl, mM	Mg, mM	SO_4, mM	K, mM	Si, μM	B, μM	Li, μM	Ca, mM	Sr, μM	Ba, μM	NH_4, μM	HS, mM	Br, μM	I, μM	$\delta^{18}O_{H2O}$, ‰ SMOW	TA, mM/kg	Measured pH	Model pH	Model PCO2 10^{-3} atmosph.
TGC-6 Reference Site																				
7.5	298	357	34.9	16.2	6.3	591	270	19	7	58	1	243	0.49	534	0	−1.71	6.9	7.6	7.13	6
42	292	356	32.9	13.2	5.8	643	260	17	7	57	1	440	0.52	506	3	n.d.	9.2	7.6	7.01	12
57.5	288	352	32.6	11.4	5.7	630	250	15	8	56	1	468	0.42	502	3	−1.92	8.3	7.5	7.03	9
72.5	288	343	32.6	12.6	5.6	627	250	22	7	57	2	558	0.32	471	4	n.d.	8.0	7.4	7.09	8
97.5	275	341	30.4	8.4	5.2	579	200	15	8	55	2	593	0.06	513	0	−1.96	10.7	7.6	6.91	17
122.5	280	337	30.3	7.5	5.1	582	220	22	8	56	2	665	0.03	477	5	n.d.	11.7	7.4	6.87	20
147.5	219	304	21.9	0	3.5	230	120	15	9	51	12	811	0	443	7	n.d.	14.8	7.7	6.73	36
172.5	242	303	24.4	0	3.5	300	140	15	11	61	15	894	0	438	8	n.d.	14.6	7.6	6.63	44
192.5	229	291	22.9	0	3.4	285	120	15	11	59	16	894	0	432	2	n.d.	14.5	7.4	6.66	42
212.5	n.d.	n.d.	n.d.	0	n.d.	n.d.	n.d	n.d.	n.d.	n.d.	n.d.	1015	0	n.d.	n.d.	n.d.	n.d.	7.4	n.d.	n.d.
232.5	228	287	23.5	0	3.0	290	120	11	13	64	19	815	0	410	8	−2.94	13.6	7.3	6.61	43
262.5	227	275	22.7	0	2.8	260	110	15	13	65	20	897	0	440	9	n.d.	12.7	7.1	6.64	38
292.5	214	276	22.0	0	2.6	248	100	12	14	66	23	1033	0	393	9	n.d.	11.7	7.0	6.65	34
312.5	209	231	20.8	0	2.4	239	100	2	14	64	19	915	0	366	1	−2.96	11.5	7.0	6.66	31
TGC-1 Odessa mud volcano																				
2.5	293	363	34.2	5.49	5.7	426	209	18	5	53	3	56	3.94	540	3	−1.76	15.9	7.3	6.97	17
12.5	278	356	32.4	1.29	5.3	385	127	14	5	58	12	86	2.75	542	1	−2.06	15.9	7.4	6.94	21
17.5	273	354	33.2	1.01	4.9	407	107	12	7	71	22	113	1.33	568	23	−2.29	13.3	7.7	6.84	24
28.0	259	335	32.2	1.60	4.3	386	83	17	10	79	27	140	0.05	541	31	n.d.	11.4	7.9	6.77	25
38.0	210	300	26.2	1.40	3.5	132	53	10	10	69	23	90	0.01	523	34	−1.89	10.3	7.9	6.81	21
49.0	249	333	32.8	0.50	4.1	138	57	10	11	88	33	110	0.00	585	8	−2.01	11.2	7.6	6.70	29
62.5	215	286	27.7	0.54	3.2	106	55	7	12	82	28	111	0.00	518	49	n.d.	10.0	7.0	6.72	26
82.0	235	328	31.7	0.00	3.4	85	49	11	15	96	33	118	0.00	600	55	n.d.	10.2	7.1	6.65	30
99.0	229	323	31.4	0.00	3.2	82	47	10	16	100	36	130	0.00	623	58	−1.63	10.0	7.1	6.65	28
115.0	227	329	31.6	0.00	3.0	88	46	11	18	104	37	149	0.00	608	62	n.d.	10.0	6.8	6.62	30
147.0	219	305	30.6	0.09	2.6	88	39	11	18	104	37	133	0.00	598	64	n.d.	8.9	6.7	6.65	25
172.0	225	326	33.5	0.01	2.7	113	44	11	20	115	38	156	0.00	599	10	−1.50	9.7	6.4	6.57	32
188.0	217	314	32.6	0.00	2.7	88	32	13	19	110	40	151	0.00	591	72	n.d.	9.0	6.4	6.62	27
217.0	197	311	24.6	0.00	2.2	102	30	13	19	102	35	131	0.00	608	71	−2.43	9.0	6.4	6.60	29
236.0	200	294	28.3	0.00	2.0	122	31	9	19	102	33	141	0.00	567	71	n.d.	9.0	6.3	6.61	28
264.0	191	281	30.1	0.00	2.2	116	30	13	19	106	34	137	0.00	564	10	−2.23	8.4	6.2	6.65	24
279.0	209	299	32.3	0.00	2.2	109	33	17	21	117	39	156	0.00	630	80	n.d.	8.3	6.4	6.61	25
295.0	202	303	31.4	0.00	2.1	114	28	13	21	113	38	163	0.00	639	80	−2.55	8.3	6.2	6.62	25
316.0	205	303	33.4	0.00	2.1	122	27	12	22	123	44	165	0.00	618	86	n.d.	8.1	6.4	6.61	25
335.5	203	315	33.0	0.00	2.1	116	27	11	22	123	44	169	0.00	680	18	n.d.	8.5	6.4	6.58	27
360.0	211	318	34.9	0.00	2.3	96	21	13	24	128	47	180	0.00	649	92	−3.05	7.2	6.5	6.64	20

Table 2. Chemical Composition of Water Masses and Pore Fluids Relevant to the Present Study

Species	Modern Black Sea[a]	Mediterranean[b]	Danube[c]	Parent Pore Fluid	TGC-1 Core Base
Cl^-	342 mM	600 mM	0.56 mM	318 mM	318 mM
Na^+	300 mM	514 mM	0.39 mM	273 mM	191–211 mM
Mg^{2+}	34.8 mM	58.5 mM	0.37 mM	31.2 mM	24.6–34.9 mM
Ca^{2+}	7.5 mM	11.2 mM	1.2 mM	6.5 mM	24.7 mM
K^+	6.3 mM	11.2 mM	25 μM	5.9 mM	2.0–2.3 mM
H_2S	0.37 mM	–	–	–	–
Si	320 μM	113 μM	100 μM[d]	106 μM	88–122 μM
B	270 μM	472 μM	0.1–18.6 μM[e]	250–259 μM	21–32 μM
Sr^{2+}	57.6 μM	100 μM	2–3 μM[d]	53.9–54.4 μM	128.4 μM
Li^+	16.8 μM	29 μM	215 nM[f]	15.5 μM	7–13 μM
Br^-	0.49 mM	–	–	–	–
NH_4	2.1 μM	–	–	–	–
I^-	0.56 μM	–	–	–	–
Ba^{2+}	446 nM	88 nM	300–450 nM[g]	187–258 nM	46.8 μM
$\delta^{18}O$	−1.65‰[h]	1.8‰[h]	−3.3‰[h]	−0.6‰	−3‰

[a] Black Sea bottom water sampled in the Sorokin Trough during cruise M52-1.
[b] The composition of eastern Mediterranean waters (S = 38.5‰ [*Sarmiento et al.*, 1988]) was calculated on the basis of the average composition of seawater at S = 35‰ [*Wilson*, 1975; *Quinby-Hunt and Turekian*, 1983].
[c] Values taken from *Berner and Berner* [1996] unless otherwise stated.
[d] *Pawellek et al.* [2002].
[e] *Lemarchand et al.* [2002].
[f] Mean of major world rivers [*Huh et al.*, 1998].
[g] *Kenison Falkner et al.* [1991].
[h] *Swart* [1991].

coefficient. In equation (1), we accounted for the effect of sediment tortuosity on molecular diffusion by applying Archie's Law [*Berner*, 1980]. Molecular diffusion coefficients for K, Na, B and Cl^- are taken from *Boudreau* [1997]. The porosity-depth profile, $\phi(x)$, is considered to be produced by steady state compaction [*Berner*, 1980] and is described by the following exponential function:

$$\phi(x) = \phi_f + (\phi_0 - \phi_f) \cdot e^{[-\phi_a \cdot x]}, \quad (2)$$

where values of porosity at the sediment surface (ϕ_0), 0.90, porosity at great sediment depth (ϕ_f), 0.67, and of the porosity-depth attenuation coefficient (ϕ_a), 0.041, have been determined for the studied sites by fitting porosity data obtained by the measurement of the sediment water content. The rate of fluid advection, $u(x)$, is treated as by *Luff and Wallmann* [2003] and is composed of the downward burial component modified by compaction and the upward component due to fluid advection:

$$u(x) = \frac{v_f \cdot \phi_f - w_0 \cdot \phi_0}{\phi(x)} \quad (3)$$

where v_f is the sedimentation rate at great depth and w_0 the upward rate of fluid flow at the seafloor. A 360 cm long sediment column was modeled, using bottom water concentrations of K^+, B, Na^+ and Cl^- as upper boundary conditions (x = 0 cm) and the concentrations of these solutes at the core base as lower boundary conditions (x = 360 cm). The sedimentation rate was varied in the range 0.005 cm a^{-1} to 0.025 cm a^{-1} which covers the sedimentation rates measured during previous cruises in the Sorokin Trough [*Woodside et al.*, 1997]. Numerical solutions to equation (1) for Na^+, B, K^+ and Cl^- were obtained using the commercial software Mathematica. We observed that the sedimentation rate has a negligible influence on the fitting procedure. Fitting the Cl^- data was problematic, due to the scatter of the Cl^- data (Figure 5). The local Cl^- minimum in correspondence to the gas hydrate layer at 260 cm depth could be due to gas hydrate dissociation during core recovery. Indeed, the profiles of other solutes (Mg^{2+}, Ca^{2+}, Sr^{2+}, Ba^{2+}, Li^+) show concentration minima centered around this depth. A satisfactory fit of the calculated Na^+, B and K^+ profiles to the field data was obtained using a seepage rate of 5 cm a^{-1} (Figure 5). This value approaches the lower end of the range of seepage rates (0–1000 cm a^{-1}) most commonly measured at cold seeps [*Tryon and Brown*, 2001; *Luff and*

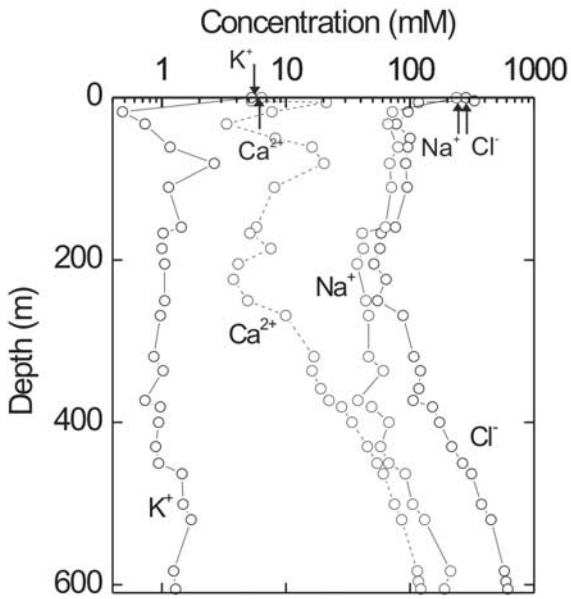

Figure 6. Concentration profiles of Ca^{2+}, Na^{+}, K^{+} and Cl^{-} at DSDP site 379 in the central Black Sea. Redrawn from *Manheim and Schug* [1978].

Wallmann, 2003] indicating that the eastern flank of the Odessa mud volcano is subject to a relatively gentle emission of fluids.

[15] The above considerations confirm that site TGC-1 is subject to fluid seepage, but do not inform us about the depth of provenance of the fluids. A strong indication arguing in favor of a very shallow source is provided by comparing the chloride content of fluids expelled at site TGC-1 with that of Black Sea pore fluids drilled at DSDP site 379 [*Manheim and Schug*, 1978] (Figure 6). The results of DSDP Leg 42A show that since the Tortonian (Late Miocene), the salinity of the Black Seawater mass has varied considerably [*Hsü*, 1978; *Manheim and Schug*, 1978]. Because the sedimentation rate in the Black Sea is relatively high (up to 90 cm per 1000 yr [*Hsü*, 1978]), sediment pore waters have retained the salinity of the overlying water mass to a very high degree. Thus the Messinian (Late Miocene) hypersaline stage of the Black Sea is recorded at site 379 by the elevated Cl^{-} concentration below 450 m depth (Figure 6). The subsequent Pliocene fresh water to brackish stage is marked by a negative shift in the Cl- profile with chloride concentrations lower than that those of modern Black Seawaters between 450 and 20 m depth (Figure 6). The final evolution to the present, brackish, water mass occurred at the end of the Limnic period (circa 9000 yBP [*Boudreau and Leblond*, 1989]) and produced the sharp increase in chlorinity in the upper 20 m of sediments. The fluids expelled from the eastern flank of the Odessa mud volcano are fresher than modern Black Sea bottom waters (Table 2), suggesting that they originate from the low-salinity interval which is located between 20 and 450 m depth at DSDP Site 379. Should the source of fluids have been deeper, the chemistry would have been influenced by the underlying high-salinity pore waters. In support of this interpretation, fluids expelled from ~3 km depth at the center of the Dvurechenskii mud volcano (located just 10 nautical miles SW of the Odessa mud volcano) are hypersaline [*Bohrmann et al.*, 2004; G. Aloisi et al., Fluid expulsion from the Dvurechenskii mud volcano (Black Sea), Part I: Fluid sources and relevance to Li, B, Sr and dissolved inorganic nitrogen cycles, submitted to *Earth and Planetary Science Letters*, 2004].

[16] The density inversion in the top 20 m at DSDP Site 379 suggests that also at site TGC-1 a density inversion could occur. This would imply a salinity contrast between the expelled, fresher fluids and the surrounding, more saline pore waters. Previous studies [e.g., *Henry et al.*, 1996] have shown that the expulsion of low-salinity fluids at mud volcanoes may trigger shallow convection, a process that is potentially widespread at cold seeps [*Tryon and Brown*, 2001; G. Aloisi et al., Chemical, biological and hydrological controls on the ^{14}C content of cold seep carbonate crusts: Numerical modeling and implications for convection at cold seeps, submitted to *Chemical Geology*, 2004]. We do not have sufficient knowledge of the chemistry and physics of site TGC-1 to understand if convection is indeed taking place there. In any case, our results suggest that convection could be common at cold seeps in the Black Sea.

[17] A depth of origin of a few hundred meters for fluids at sites TGC-1 is unusually shallow for mud volcanic fluids which commonly originate from several km depth [*Martin et al.*, 1996; *Kopf and*

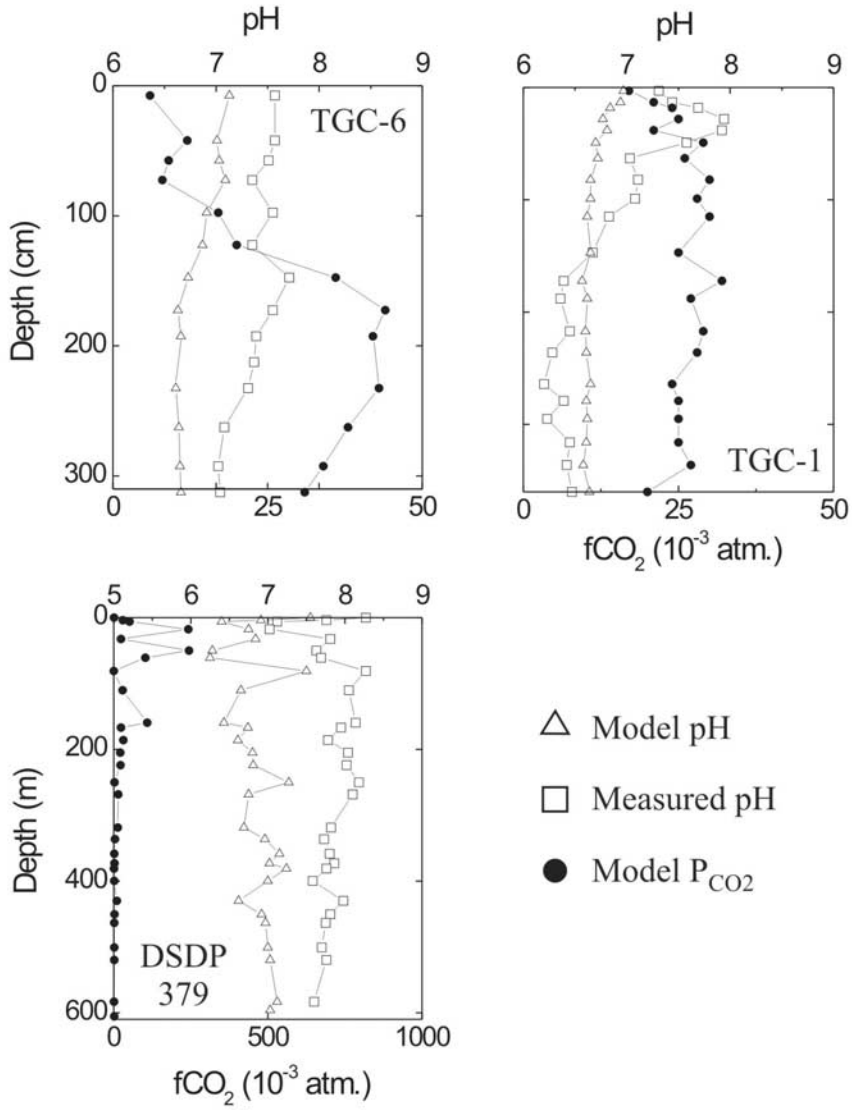

Figure 7. Measured and calculated pH profiles in cores TGC-1, TGC-6 and DSDP site 379 (DSDP data from *Manheim and Schug* [1978]) and calculated profiles of partial pressure of CO_2 (PCO_2).

Deyhle, 2002]. On the basis of seismic evidence, the Odessa mud volcano and the mud diapir beneath it have roots much in excess of a few hundred meters [*Krastel et al.*, 2004]. Therefore a specific fluid expulsion mechanism probably related to the mud intrusion/expulsion process, but not implying a deep fluid source, has to be considered. Seismic section 02-003 (Figure 2) shows that the sedimentary strata surrounding the diapiric intrusion are bent upward by the emplacement of the mud diapir. Furthermore, the decrease in thickness of the top few hundred meters of sediments approaching the diapiric intrusion shows that they have undergone consolidation and, consequently, expulsion of fluids. Core TGC-1 lies on top of this compacted sedimentary section which is the most probable source for the fresh, shallow fluids seeping at this site.

5.2.2. Evidence for a Sedimentary Li and B Sink Through Detrital Silicate Mineral Alteration

[18] In this section we investigate the chemistry of the fluids expelled at site TGC-1 in order to better

characterize the diagenetic processes taking place in shallow Black Sea sediments. In particular, we want to understand the fate of Li and B in the diagenetic environment of shallow Black Sea sediments. Due to the complex hydrological history of the Black Sea, the chemical effect of diagenesis will be superimposed on a parent fluid (hereafter: "parent pore fluid") the chemistry of which likely was very different from that of modern Black Seawater. Thus, to decipher the diagenesis-related chemical signal, the chemistry of the parent pore fluid has to be obtained and compared with that of fluids in the lower part of core TGC-1.

[19] The parent pore fluid was formed when the Black Sea had a lower salinity than at present. During this period, the chemistry of Black Seawaters was the result of mixing between river inputs (mainly from the Danube River [*Özsoy and Ünlüata*, 1997]) and Mediterranean inputs from the Bosporus Strait. If Cl^- behaves conservatively in the first few hundred meters of sediments, the Cl^- concentration at the base of core TGC-1 can be considered the result of a simple two end-member mixing between Danube river waters and Mediterranean waters. However, because gas hydrate crystals are present in core TGC-1, the measured Cl^- data may differ from the in situ concentration, if gas hydrate destabilization during core recovery has significantly diluted pore fluids [*Hesse*, 2003]. Small Cl^- minima at 147 and 264 cm depth occur in correspondence to gas hydrate layers (Figure 4), suggesting that gas hydrate decomposition during core recovery may have affected the Cl^- profile at these depths [*Bohrmann et al.*, 2004]. Clearly, however, the trends of decreasing Cl^- and $\delta^{18}O_{H2O}$ with depth are not related to dissociation of gas hydrates during core recovery which would result in a general increase in pore water $\delta^{18}O_{H2O}$. Rather, they reflect upward seepage of a Cl^- and ^{18}O-depleted fluid. Thus we consider the two end-member mixing model applicable and estimate that the Cl^- concentration at the base of core TGC-1 (318 mM) is obtained by mixing 47% of Danube river waters with $[Cl^-]$ = 0.56 mM with 53% of Mediterranean waters with $[Cl^-]$ = 600 mM (see Table 2 for Mediterranean and Danube river chemistry). Applying this mixing ratio we calculate the chemistry of the parent pore fluid (Table 2). The $\delta^{18}O$ of the Black Sea in periods of no exchange with Mediterranean waters is estimated to have been −3.3‰ [*Swart*, 1991]. Mixing of Mediterranean waters ($\delta^{18}O$ = 1.8‰ SMOW [*Pierre*, 1999]) and fresh Black seawaters of riverine origin in the above calculated proportions yields a water mass having a $\delta^{18}O$ of −0.6‰.

[20] In the bottom meter of the core, concentration profiles of Cl^-, Na^+, Mg^{2+}, B, K^+, Li^+ and Si are roughly constant, indicating that diffusion from seawater has not affected their concentration at depths greater than 250 cm. Compared to the parent pore fluid, the fluid at the base of core TGC-1 is strongly depleted in Na^+, K^+, Li^+, and B (Table 2). The Mg^{2+} and Si concentrations are comparable to those of the parent pore fluid. Because concentrations of Ca^{2+}, Sr^{2+} and Ba^{2+} in the lower part of the core are not constant but increase with depth, the concentration of these solutes in the source area of fluids is likely greater than that at the base of core TGC-1. Similarly, $\delta^{18}O_{H2O}$ values decrease with depth in the lower part of the core suggesting even lower $\delta^{18}O$ values at depth. We have observed that diagenetic processes in shallow Black Sea sediments are a significant Li and B sink. We now investigate the possible nature of this diagenesis by looking more carefully at the chemistry of the expelled fluids.

5.2.2.1. Na^+, Mg^{2+}, Ca^{2+}, K^+, Li^+, and B

[21] Generally, fluids expelled at cold seeps contain less Ca^{2+} than seawater due to carbonate precipitation processes which are common in anoxic sediments [*Martin et al.*, 1996; *Wallmann et al.*, 1997; *Luff and Wallmann*, 2003]. The fluid seeping at site TGC-1, however, contains considerably more Ca^{2+} than the parent pore fluid, indicating that diagenetic processes result in a net production of calcium in the fluid source area. The excess Ca^{2+} could be provided by the dissolution of carbonate minerals such as calcite

($CaCO_3$) and dolomite ($CaMg(CO_3)_2$) [*Martin et al.*, 1996]:

$$CaCO_3 + CO_2 + H_2O \rightarrow Ca^{2+} + 2HCO_3^-, \quad (4)$$

$$CaMg(CO_3)_2 + 2CO_2 + 2H_2O \rightarrow Ca^{2+} + Mg^{2+} + 4HCO_3^-. \quad (5)$$

However, these processes do not explain the strong K^+ and Na^+ depletion of fluids expelled at site TGC-1 compared to the parent pore fluid. *Manheim and Schug* [1978] propose that Ca^{2+}, Mg^{2+} and K^+ in shallow Black Sea sediments are controlled by silicate diagenesis and propose that volcanic ash is the source of silicate [*Gieskes*, 1981; *Egeberg et al.*, 1990; *Martin et al.*, 1996]:

$$\text{volcanic ash} + Mg^{2+} + K^+ + Na^+ + H_2O \rightarrow \text{smectite} + Ca^{2+}. \quad (6)$$

However, detailed lithological investigations of sediments recovered during DSDP Leg 42A failed to find volcanic ash layers or a volcanic basement at DSDP site 379 [*Shimkus et al.*, 1978; *Trimonis et al.*, 1978]. In fact, with the exception of low quantities of Neogene volcanic ashes found at Site 380 near the Bosporus, sediments investigated during DSDP Leg 42A are free of volcanic ashes. It is clear that an alternative source of silicates has to be present to account for the observed chemical trends. Detrital silicate minerals are abundant in the sediments drilled during DSDP Leg 42A [*Stoffers and Müller*, 1978]. At Site 379, quartz and feldspars make up up to 60 wt-% of the sediment. Amongst the feldspars, plagioclase, the calcium-bearing feldspar, is the most abundant and accounts for up to 30 wt-% of the sediment. During subaerial weathering reactions, Ca-bearing silicates react with CO_2, dissolve, form clay minerals and liberate calcium and bicarbonate:

$$2CO_2 + 3H_2O + CaAl_2Si_2O_8(\text{anorthite}) \rightarrow Ca^{2+} + 2HCO_3^- + Al_2Si_2O_5(OH)_4(\text{kaolinite}). \quad (7)$$

[22] Depending on the abundance of the different silicate minerals in the parent sediment and on their cationic composition, a large number silicate alteration reactions are possible, which result in the formation of different authigenic clay minerals [*Stumm and Morgan*, 1996]. Notwithstanding, the low-temperature weathering of Ca-bearing silicate minerals always results in the release of Ca^{2+} and the precipitation of authigenic clay minerals. By analogy to volcanic ash alteration, during submarine silicate mineral weathering processes authigenic clays would likely be a sink for Na^+, K^+, Li^+ and B. Thus detrital silicate mineral dissolution and authigenic clay mineral formation is entirely consistent with the distribution of Na^+, Mg^{2+}, Ca^{2+}, K^+, Li^+ and B in shallow Black Sea sediments. Because reaction 7 consumes water, extensive alteration of detrital silicate minerals may lead to an increase in pore water salinity, similar to what occurs during extreme events of volcanic ash alteration [*Gieskes and Lawrence*, 1981; *Staudigel et al.*, 1995]. Should this be the case, it would imply that the parent pore fluid is less saline than the parent pore fluid composition we estimated above (Table 2). However, since water consumption affects the concentration of all solutes, the described pattern of solute enrichment and depletion would still occur.

5.2.2.2. $\delta^{18}O_{H2O}$

[23] Numerous diagenetic processes alter the oxygen isotope composition of pore fluids. The dehydration and transformation of clay minerals release structurally bound ^{18}O-rich water resulting in low-salinity and ^{18}O-rich pore fluids [*Savin and tiftein*, 1970; *Yeh and Savin*, 1977]. Similarly, the destabilization of gas hydrate deposits releases ^{18}O-rich water which dilutes pore fluids [*Hesse*, 2003]. On the basis of the ^{18}O depletion of the expelled fluids, these processes can be discarded as major contributors to diagenesis in the fluid source area. The retention of dissolved ions and $H_2{}^{18}O$ in clay mineral membranes can produce low-salinity, ^{18}O-poor fluids through a process called membrane filtration [*Hanshaw and Coplen*, 1973]. However, the efficiency of membrane filtration is highly dependent on the state of compaction, and it is improbable that the shallow sediments of the source have sufficiently low porosity to act as semi-permeable membranes. Due to the low temperature at which subaerial weathering reactions take place, ^{18}O is concentrated in the authigenic clay minerals [*Hoefs*, 1997]. Thus the observed ^{18}O depletion in

the expelled fluids supports the hypothesis that detrital silicate minerals are being weathered in shallow Black Sea sediments. In addition, the geochemical indication for a low-temperature diagenesis confirms the shallow provenance of the expelled fluids inferred on the basis of the salinity-depth profile at DSDP Site 379.

5.2.2.3. Ba^{2+} and Sr^{2+}

[24] Ba is present in marine sediments mostly as 'bio-barite' ($BaSO_4$) formed in sedimentary basins overlain by biologically highly productive water columns. Sr can substitute effectively for Ca in carbonates and for Ba in barite [*Baker et al.*, 1982; *Averyt and Paytan*, 2003]. Thus these cations are susceptible of being redistributed between fluids and authigenic phases during precipitation/dissolution processes involving these minerals [*Baker et al.*, 1982; *Torres et al.*, 1996]. In marine sediments, an important source of Ba^{2+} and Sr^{2+} is the dissolution of 'bio-barite', below the depth of sulfate depletion [*Torres et al.*, 1996]. A deeper source of Ba^{2+} and Sr^{2+} possibly is the alteration of deeper sedimentary rocks, because these elements are abundant in sedimentary material. It is plausible that the elevated Ba^{2+} content of fluids at site TGC-1 derives from dissolution of bio-barite. However, this process cannot be the sole source of Sr^{2+}, given that the Sr/Ba ratio in bio-barite is only 0.032 [*Averyt and Paytan*, 2003]. The subaerial weathering of silicate minerals is a major source of Sr^{2+} to the ocean [*Wallmann*, 2001]. Thus we believe that, if silicates are being weathered in Black Sea sediments, they may add Sr^{2+} to pore waters and contribute in producing the observed elevated Sr^{2+} concentration. Elevated Sr^{2+} concentration in fluids expelled from mud volcanoes of the Barbados accretionary prism, however, are interpreted as due to Sr^{2+} release during the recrystallization of carbonates [*Martin et al.*, 1996] and it is possible that also this process is taking place in Black Sea sediments.

5.2.3. Submarine Weathering of Detrital Silicate Minerals Favored by Low pH

[25] The dissolution rate of silicate minerals is controlled by surface reactions [*Stumm and Morgan*, 1996]. Protonation of O and OH lattice sites on mineral surfaces produces a net positive charge facilitating the detachment of cationic surface groups and their release to the solution. Thus the dissolution rate of silicate minerals is favored at low pH (a similar effect occurs at high pH, due to net negative surface charge). In support of this observation, the partial pressure of CO_2 (P_{CO2}) in soils experiencing silicate weathering processes, is typically several hundred times higher than the atmospheric value of $\approx 0.35 \times 10^{-3}$ atmospheres. Thus knowledge of the pH and the P_{CO2} in Black Sea sediments is necessary in order to understand if detrital silicates are being weathered there.

[26] Measured pH values in cores TGC-1 and TGC-6 fall from 7.3 and 7.6 at the core top to 6.5 and 7.0 at the core bottom, respectively (Figure 7). These values are lower than seawater pH ($\approx$8.1) and somewhat lower than measured pH values in continental slope sediments [*Pfeifer et al.*, 2002] or pH values obtained by diagenetic modeling of deep marine sediments [*Luff et al.*, 2000] and cold seep sediments [*Luff and Wallmann*, 2003]. pH measurements carried out on deep marine sediments, however, are not reliable. During sampling and pore water extraction, CO_2 degasses from pore fluids due to pressure decrease. Thus onboard pH measurements typically overestimate in situ pH values by as much as 1–1.5 units. In this section we estimate the in situ sediment pH in cores TGC-1 and TGC-6, as well as DSDP site 379, by using a simple chemical model that uses total alkalinity and dissolved calcium concentrations and makes assumptions on the fluid-solid carbonate equilibrium.

[27] Black Sea sediments contain abundant detrital and biogenic calcite [*Stoffers and Müller*, 1978] such that pore fluids can be considered to be in chemical equilibrium with respect to this mineral. Thus the concentration of the carbonate ion can be obtained by imposing a saturation state, Ω, equal to 1 in the expression defining the saturation state of fluids with respect to calcite:

$$\Omega = \frac{C_{Ca^{2+}} \cdot C_{CO_3^{2-}}}{K^*_{sp}}. \quad (8)$$

The stoichiometric solubility product of calcite, K^*_{sp}, is obtained as a function of temperature,

salinity and pressure [*Zeebe and Wolf-Gladrow*, 2001] and is corrected to account for the deviation of pore fluid chemistry from that of seawater according to P. Tishchenko et al. (Dissociation constants of carbonic acid and solubility of calcium carbonate in pore waters of anoxic marine sediments, submitted to *Geochimica Cosmochimica Acta*, 2004) (hereinafter referred to as Tishchenko et al., submitted manuscript, 2004). The total alkalinity can be measured reliably in sediment pore waters because it is a conservative quantity and is not affected by sediment degassing. In a simplified treatment of total alkalinity, *Zeebe and Wolf-Gladrow* [2001] define a practical alkalinity for seawater (PA) equal to

$$PA = \left[HCO_3^-\right] + 2\cdot\left[CO_3^{2-}\right] + \left[B(OH)_4^-\right] + [OH^-] - [H^+]. \tag{9}$$

In pore waters of anoxic sediments, dissolved sulfide may be present in high concentrations such that the HS^- ion can contribute significantly to the total alkalinity. We thus define a practical alkalinity for anoxic sediments, PA_{an}:

$$PA_{an} \approx TA = \left[HCO_3^-\right] + 2\cdot\left[CO_3^{2-}\right] + \left[B(OH)_4^-\right] + [HS^-] + [OH^-] - [H^+]. \tag{10}$$

To obtain the concentration of H^+ ions we set up a system of 8 equations comprising the above definition of PA_{an}, the mass balances for the borate and sulfide systems and the mass action laws for the carbonate, borate and sulfide systems and for the dissociation of water:

$$\begin{aligned} \Sigma B(OH)_4 &= \left[B(OH)_3\right] + \left[B(OH)_4^-\right] \\ \Sigma H_2S &= [HS^-] + [H_2S] \\ K_1^* = \frac{[H^+]\cdot\left[HCO_3^-\right]}{[CO_2]} \qquad K_2^* &= \frac{[H^+]\cdot\left[CO_3^{2-}\right]}{\left[HCO_3^-\right]} \\ K_B^* &= \frac{[H^+]\cdot\left[B\left(OH_4^-\right)\right]}{\left[B(OH)_3\right]} \\ K_S^* &= \frac{[HS^-]\cdot[H^+]}{[H_2S]} \\ K_W^* &= [H^+]\cdot[OH^-] \end{aligned} \tag{11}$$

where $\Sigma B(OH)_4$ and ΣH_2S are the total dissolved borate and sulfide, respectively. The stoichiometric equilibrium constants for the dissociation of carbonic, boric and sulfidic acid and of water, K_1^* and K_2^*, K_B^*, K_S^* and K_W^*, respectively, are obtained as a function of temperature, salinity and pressure [*Zeebe and Wolf-Gladrow*, 2001]. In addition, K_1^* and K_2^* were corrected to account for the deviation of pore fluid chemistry from that of seawater according to Tishchenko et al. (submitted manuscript, 2004). The dissolved calcium, $\Sigma B(OH)_4$ and ΣH_2S concentrations and the total alkalinity are taken from measured data at sites TGC-1 and TGC-6 (Table 1). *Manheim and Schug* [1978] present dissolved Ca and total alkalinity data for DSDP Site 379. However, they do not report dissolved ΣH_2S and $\Sigma B(OH)_4$ concentrations. Nevertheless, on the basis of the absence of H_2S and dissolved B in the lower part of core TGC-1, we consider that the CO_3^{2-} and HCO_3^- ions are major contributors to total alkalinity in Black Sea sediments deeper than a few meters. Thus we set the concentrations of ΣH_2S and $\Sigma B(OH)_4$ equal to 0 when calculating the pH at DSDP Site 379. The system of 8 equations and 8 unknowns ($[CO_2]$, HCO_3^-, $B(OH)_3$, $B(OH)_4^-$, HS^-, H_2S, OH^-, H^+]) was solved numerically using the FindRoot function implemented in the commercial software Mathematica. The pH is then calculated from the concentration of $[H^+]$:

$$pH = -\log[H^+]. \tag{12}$$

The P_{CO2} is obtained from the concentration of CO_2 and applying Henry's Law:

$$P_{CO2} \approx f_{CO2} = \frac{[CO_2]}{K_0^*}, \tag{13}$$

where K_0^*, Henry's constant, is calculated as a function of temperature and salinity and f_{CO2}, the fugacity of CO_2, can be considered a good approximation of P_{CO2} [*Zeebe and Wolf-Gladrow*, 2001].

[28] Our results have important implications regarding the stability of detrital silicate minerals in Black Sea sediments. Similar to the pH values measured on board, calculated pH values in reference core TGC-6 also decrease with depth (Figure 7). However, they are up to 1 pH unit lower than measured values and reach a minimum

of 6.6 in the lower part of the core. At the Odessa seepage site (core TGC-1), the pH profile is convex upward and pH values decrease from 7 at the top of the core to 6.62 at the bottom. In contrast to the measured values, calculated pH values only show a very small maximum in correspondence to the depth of complete sulfate depletion. It is probable that the measured pH values strongly overestimate the in situ pH in this depth interval where enhanced CO_2 degassing probably occurs due to production of dissolved inorganic carbon through anaerobic methane oxidation and subsequent pressure release during sampling. Surprisingly, in the lower part of core TGC-1, measured pH values underestimate the calculated pH by as much as 0.45 pH units (Figure 7). Given that up to 100 μM Fe^{2+} are present below 140 cm depth in this core (data not shown), this pH anomaly is likely due to release of protons during post sampling oxidation of Fe^{2+} by oxygen:

$$4Fe^{2+} + O_2 + 10H_2O + \rightarrow 4Fe(OH)_3 + 8H^+. \quad (14)$$

Nevertheless, in both cores TGC-1 and TGC-6, decreasing pH values with depth suggests that fluids at depth are characterized by a low pH. Consistent with the pH trends in cores TGC-1 and TGC-6, the calculated pH at DSDP Site 379 is as much as 1.7 units lower than the measured values reported by *Manheim and Schug* [1978], attaining a minimum of 6.2 in the fresh pore water interval. In a similar attempt to obtain realistic in situ pH values for Black Sea sediments cored during DSDP Leg 42A, *Manheim and Schug* [1978] calculated a pH as low as 5.87 in the hypersaline playa deposits of DSDP Site 380. Thus the unusually low pore water pH of Black Sea sediments is not restricted to the low-salinity interval but extends into the underlying hypersaline sediments, possibly representing a widespread characteristic of Black Sea sediments. Such low pH values are coupled to elevated P_{CO2} levels. In cores TGC-1 and TGC-6, P_{CO2} levels range from 17 to 44 $\times$ 10^{-3} atmospheres, whereas at DSDP Site 379 they attain 240 $\times$ 10^{-3} atmospheres (Figure 7), suggesting conditions comparable to those present in soils undergoing silicate weathering processes. Both the low pH and the elevated P_{CO2}, together with the elemental and isotopic signature of pore waters discussed in section 5.2.2, provide ample evidence that the submarine weathering of silicates is driving diagenesis in the top few hundred meters of Black Sea sediments. The origin of such a low pH in Black Sea sediments, however, has to be explained.

[29] *Jørgensen et al.* [2001] have shown that in the Black Sea dissolved sulfate is consumed in the top few meters of sediments both in continental shelf environments and in the abyssal plain. In marine sediments, after complete sulfate depletion, organic matter degradation proceeds via methanogenesis, producing methane and carbon dioxide [*Claypool and Kaplan*, 1974]:

$$2C(H_2O) \Rightarrow CH_4 + CO_2. \quad (15)$$

In turn, production of CO_2 through methanogenesis lowers the pH of pore fluids. Thus the potential for a sediment to host low-pH pore waters depends on the organic matter accumulation rate. High organic matter accumulation rates have characterized the Black Sea in the past, leading to the deposition of numerous sapropels throughout the Plio-Pleistocene [*Stoffers and Müller*, 1978], likely favoring CO_2 production though methanogenesis. Indeed, evidence for continued microbial activity below the depth of sulfate depletion is provided by the high concentration of species produced during organic matter degradation processes in core TGC-1. In this core, concentrations of NH_4, Br^- and I^- are up to 10 times higher than at the reference site and Br^-/Cl^- and I^-/Cl^- ratios are elevated suggesting transport of NH_4, Br^- and I^- from deeper sediment intervals. In addition, high NH_4 concentrations (up to 11.4 mM at site 380) and elevated Br^-/Cl^- ratios have been observed at DSDP Site 379 [*Manheim and Schug*, 1978; *Shishkina*, 1978]. The conditions favoring organic matter accumulation in marine sediments are controversial. Most authors think that high organic matter accumulation rates are favored by elevated bulk sedimentation rates and high primary productivity in the water column [*Müller and Suess*, 1979; *Betts and Holland*, 1991]. Other authors, however, propose that water column anoxia may limit organic matter degradation in

the water column, increasing the organic matter flux to the seafloor [*Lasaga and Ohmoto*, 2002]. *Calvert et al.* [1987] and *Arthur and Dean* [1988] propose the latter mechanism could enhance organic matter accumulation rates in the Black Sea (currently the upper 150 m of the Black Seawater column are oxygenated, while the underlying water masses are anoxic [*Özsoy and Ünlüata*, 1997]). In any case, CO_2 production through methanogenesis is the best explanation for the low pH of Black Sea pore waters examined in the present study.

5.2.4. Possible Implications for the Li and B Cycles

[30] Present knowledge of the marine Li cycle predicts that the magnitude of the principal sources (hydrothermal fluids, rivers and cold seepage) exceeds that of sinks (water column adsorption and low-temperature alteration of basaltic rocks) by a factor of ≈2 [*Stoffyn-Egli and Mackenzie*, 1984; *Zhang et al.*, 1998]. A lack of isotopic mass balance also exists because the preferential ^{6}Li incorporation into altered basalts at low temperature is not sufficient to account for the ^{7}Li enrichment of seawater (δ^6Li = −32.3‰) compared to hydrothermal fluids (δ^6Li = −6 to −11‰) and rivers (δ^6Li ≈ −23‰) [*Chan et al.*, 1992; *Huh et al.*, 1998]. Thus a balanced Li cycle implies a smaller than estimated hydrothermal flux, the existence of one or more additional Li sinks concentrating ^{6}Li [*Chan et al.*, 1992; *Huh et al.*, 1998], or both. In the sediment, the alteration of volcanic ash at low temperature likely accounts for only ≈5% of the total Li inputs to the ocean [*Zhang et al.*, 1998]. Should the silicate weathering process we describe from the Black Sea be common in marine environments, it would represent a supplementary Li sink. The environments favoring the submarine weathering of silicate minerals would have to be rich in organic matter and would have to receive abundant, fresh (reactive), detrital silicates from the continent. Such conditions are met in highly productive continental shelf environments located near young, growing mountain ranges where enhanced erosion rates minimize the transit time of siliciclastic detritus from the continent to the shelf environment and clastic sedimentation rates are high. In this scenario, the seafloor would act as a source of Li at convergent margins where most of the fluid expulsion activity occurs, and as a Li sink in organic matter-rich shallow environments and in portions of the seafloor underlain by volcanic ash deposits. Because the shallow marine environment has not been considered yet as a potential player in the marine Li cycle, the submarine weathering of silicates would represent a supplementary Li sink that could help balance the marine Li budget. Furthermore, since authigenic clays preferentially incorporate ^{6}Li [*Chan et al.*, 1992], this would also help solve the apparent lack of isotopic mass balance in the Li cycle.

[31] Recent mass balance considerations for the marine B cycle conclude that the marine B and B isotope budgets are balanced [*Lemarchand et al.*, 2002]. Sedimentary diagenetic processes, however, have not been included in mass balance considerations for the B cycle yet [*Seyfried et al.*, 1984; *You et al.*, 1993; *Vengosh et al.*, 1991; *Smith et al.*, 1995; *Lemarchand et al.*, 2002]. Because Li and B behave similarly during diagenesis, and because the residence time of these two elements in the ocean is of the same order of magnitude, diagenetic processes relevant to the Li cycle should also affect the B cycle. For example, the low-temperature alteration of volcanic ash, which is a Li sink [*Zhang et al.*, 1998], is probably also a B sink. Similarly, the submarine weathering of detrital silicates could have an impact on the B cycle, since this process is an effective B sink. Thus, should the submarine weathering of detrital silicates be widespread, it would result in an apparent imbalance in the B cycle.

[32] As an addition, we briefly comment on the impact that our results could have on the marine K budget, which has received less attention in the literature than that of Li and B. Potassium is one of the main dissolved components in seawater which poses most problems in terms of its budget [*Berner and Berner*, 1996]. This is because no important removal mechanism has been quantified. It is thought that marine sediments

possibly constitute an important K sink through volcanic ash alteration processes, fixation onto illite or reverse weathering reactions [*Sayles*, 1979, 1981; *Rude and Aller*, 1994]. It is clear, on the basis of the strong K depletion observed in Black Sea pore fluids (Figure 5), that the submarine weathering of silicates could play a role also in the marine K cycle, if future research will prove this process to be common.

6. Conclusions

[33] Our study of fluids expelled at the Odessa mud volcano describes a previously poorly characterized shallow diagenetic environment. At the eastern flank of the mud volcano, fluids originate from shallow sediments surrounding the underlying mud diapir and are expelled through diapirism-induced compaction. The fluids are enriched in Ca^{2+} and Sr^{2+} and depleted in Na^{+}, K^{+}, Li^{+}, B and ^{18}O, indicating that low-temperature dissolution of plagioclase feldspars and formation of authigenic clays is taking place. An unusually low pH (≈6) and P_{CO2} levels several hundred times higher than in the atmosphere characterize this diagenetic environment providing conditions similar to those that promote silicate mineral weathering processes in subaerial soils. In shallow Black Sea sediments, the weathering of detrital silicate minerals is promoted by elevated organic matter accumulation rates which enhance CO_2 production through methanogenesis. Should these conditions be common in shallow, organic matter-rich continental shelf environments the submarine weathering of silicate minerals could represent a previously unaccounted Li and B sink which could help balance the Li and Li isotope budgets, but would imply an apparent imbalance in the marine B cycle.

Acknowledgments

[34] The captains and crew members of the research vessel Meteor provided helpful assistance at sea, their work is greatly appreciated. A special thank goes to Bettina Domeyer, Anke Bleyer and Kristin Naβ for having carried out the analytical work on board of the Meteor and at the shore based Geomar laboratories. Funding for this study was provided by the Deutsche Forschungsgemeinschaft (DFG) grant Sn 114/11-1. The study was also supported by grant 03G0566A (collaborative project Omega) of the Federal Ministry of Education and Research (BMBF, Bonn). This is publication GEOTHECH nr. of the GEOTECHNOLOGIEN program of the BMBF and the DFG. We are grateful to two anonymous reviewers for having critically reviewed this manuscript.

References

Aloisi, G., K. Wallmann, S. M. Bollwerk, A. Derkachev, G. Bohrmann, and E. Suess (2004), The effect of dissolved barium on biogeochemical processes at cold seeps, *Geochim. Cosmochim. Acta*, in press.

Anderson, M. A., P. M. Bertsch, and W. P. Miller (1989), Exchange and apparent fixation of lithium in selected soils and clay minerals, *Soil Sci.*, *148*, 46–52.

Arthur, M., and W. E. Dean (1988), Organic-matter production and preservation and evolution of anoxia in the Holocene Black Sea, *Paleoceanography*, *13*(4), 395–411.

Averyt, K. B., and A. Paytan (2003), Empirical partition coefficients for Sr and Ca in marine barite: Implications for reconstructing seawater Sr and Ca concentrations, *Geochem. Geophys. Geosyst.*, *4*(5), 1043, doi:10.1029/2002GC000426.

Baker, P. A., J. M. Gieskes, and H. Elderfield (1982), Diagenesis of carbonates in deep-sea sediments—Evidence from Sr/Ca ratios and interstitial dissolved Sr^{2+} data, *Sediment. Petrol.*, *52*, 71–82.

Berner, R. (1980), *Early Diagenesis: A Theoretical Approach*, *Princeton Series in Geochemistry*, Princeton Univ. Press, Princeton, N. J.

Berner, E. K., and R. Berner (1996), *Global Environment: Water, Air, and Geochemical cycles*, Prentice-Hall, Old Tappan, N. J.

Betts, J. N., and H. D. Holland (1991), The oxygen content of ocean bottom waters, the burial efficiency of organic carbon, and the regulation of atmospheric oxygen, *Palaeogeogr. Palaeoclimatol. Palaeoecol.*, *97*, 5–18.

Bohrmann, G., and S. Schenck (2002), RV Meteor Cruise Report M52/1, *GEOMAR Rep. 108*, Kiel, Germany.

Bohrmann, G., et al. (2004), Mud volcanoes and gas hydrates in the Black Sea—New data from Dvurechenskii and Odessa mud volcanoes, *Geo Mar. Lett.*, *23*(3–4), 239–249.

Boudreau, B. P. (1997), *Diagenetic Models and Their Implementation—Modeling Transport and Reaction in Aquatic Sediments*, Springer-Verlag, New York.

Boudreau, B. P., and P. H. Leblond (1989), A simple evolutionary model for water and salt in the Black Sea, *Paleoceanography*, *4*, 157–166.

Calvert, S. E., J. S. Vogel, and J. R. Southon (1987), Carbon accumulation rates and the origin of the Holocene sapropel in the Black Sea, *Geology*, *15*, 918–921.

Chan, L.-H., and M. Kastner (2000), Lithium isotopic compositions of pore fluids and sediments in the Costa Rica subduction zone: Implications for fluid processes and sediment contribution to the arc volcanoes, *Earth Planet. Sci. Lett.*, *183*, 275–290.

Chan, L. H., J. M. Edmond, G. Thompson, and K. Gillis (1992), Lithium isotopic composition of submarine basalts: Implications for the lithium cycles in the oceans, *Earth Planet. Sci. Lett.*, *108*, 151–160.

Chan, L. H., J. M. Edmond, and G. Thompson (1993), A lithium isotope study of hot springs and metabasalts from mid-oceanic ridge hydrothermal systems, *J. Geophys. Res.*, *98*, 9653–9659.

Chan, L. H., J. M. Gieskes, C. F. You, and J. M. Edmond (1994), Lithium isotope geochemistry of sediments and hydrothermal fluids of the Guaymas Basin, Gulf of California, *Geochim. Cosmochim. Acta*, *58*, 4443–4454.

Claypool, G. W., and I. R. Kaplan (1974), The origin and distribution of methane in marine sediments, in *Natural Gases in Marine Sediments*, edited by I. R. Kaplan, pp. 99–139, Plenum, New York.

Deyhle, A., and A. Kopf (2002), Strong B enrichment and anomalous δ^{11}B in pore fluids from the Japan Trench forearc, *Mar. Geol.*, *183*, 1–15.

Dickson, A. D. (1993), pH buffers for sea water media based on the total hydrogen ion concentration scale, *Deep Sea Res., Part I*, *40*, 107–118.

Egeberg, P. K., and Scientific Party of Leg 113 (1990), Unusual composition of pore water found in the Izu-Bonin forearc sedimentary basin, *Nature*, *344*, 215–218.

Gieskes, J. M. (1981), Deep sea drilling interstitial water studies: Implications for chemical alteration of the ocean crust, layers I and II, in *The DSDP: A Decade of Progress*, edited by J. E. Warme, R. G. Douglas, and E. L. Wintere, pp. 149–169, SEMP (Soc. for Sediment. Geol.), Tulsa, Okla.

Gieskes, J. M., and J. R. Lawrence (1981), Alteration of volcanic matter in deep-sea sediments: Evidence form the chemical composition of interstitial waters from deep sea drilling cores, *Geochim. Cosmochim. Acta*, *45*, 1687–1703.

Hanshaw, B. B., and T. B. Coplen (1973), Ultrafiltration by compacted clay membrane—II: Sodium ion exchange at various ionic strengths, *Geochim. Cosmochim. Acta*, *37*, 2311–2327.

Henry, P., et al. (1996), Fluid flow in and around a mud volcano field seaward of the Barbados accretionary wedge: Results from Manon cruise, *J. Geophys. Res.*, *101*(B9), 20,297–20,323.

Hesse, R. (2003), Pore water anomalies of submarine gas-hydrate zones as tool to assess hydrate abundance and distribution in the subsurface: What have we learned in the past decade?, *Earth Sci. Rev.*, *61*, 149–179.

Hoefs, J. (1997), *Stable Isotope Geochemistry*, 4th ed., Springer-Verlag, New York.

Hsü, K. (1978), Stratigraphy of the lacustrine sedimentation in the Black Sea, *Initial Rep. Deep Sea Drill. Proj.*, *42*, 509–524.

Huh, Y., L.-H. Chan, L. Zhang, and J. M. Edmond (1998), Lithium and its isotopes in major world rivers: Implications for weathering and the oceanic budget, *Geochim. Cosmochim. Acta*, *62*(12), 2039–2051.

Ishikawa, T., and E. Nakamura (1993), Boron isotope systematics of marine sediments, *Earth Planet. Sci. Lett.*, *117*, 567–580.

Jørgensen, B. B. (1982), Mineralization of organic matter in the seabed—The role of sulfate reduction, *Nature*, *296*, 643–645.

Jørgensen, B. B., A. Weber, and J. Zopfi (2001), Sulfate reduction and anaerobic methane oxidation in Black Sea sediments, *Deep Sea Res., Part I*, *48*, 2097–2120.

Kastner, M. (1981), Authigenic silicates in deep-sea sediments: Formation and genesis, in *The Sea*, vol. 7, *The Oceanic Lithosphere*, pp. 915–980, John Wiley, New York.

Kenison Falkner, K., D. J. O'Neill, J. F. Todd, W. S. Moore, and J. M. Edmond (1991), Depletion of barium and radium-226 in Black Sea surface waters over the past thirty years, *Nature*, *350*, 491–494.

Kopf, A., and A. Deyhle (2002), Back to the roots: Boron geochemistry of mud volcanoes and its implications for mobilization depth and global B cycling, *Chem. Geol.*, *192*, 195–210.

Krastel, S., V. Spiess, M. Ivanov, W. Weinrebe, G. Bohrmann, P. Shashkin, and F. Heidersdorf (2004), Acoustic investigations of mud volcanoes in the Sorokin Trough, Black Sea, *Geo Mar. Lett.*, *23*(3–4), 230–238.

Lasaga, A., and H. Ohmoto (2002), The oxygen geochemical cycle: Dynamics and stability, *Geochim. Cosmochim. Acta*, *66*(3), 361–381.

Lemarchand, D., J. Gaillardet, É. Lewin, and C. J. Allègre (2002), Boron isotope systematics in large rivers: Implications for the marine boron budget and paleo-pH reconstruction over the Cenozoic, *Chem. Geol.*, *190*, 123–140.

Luff, R., and K. Wallmann (2003), Fluid flow, methane fluxes, carbonate precipitation and biogeochemical turnover in gas hydrate-bearing sediments at Hydrate Ridge, Cascadia Margin: Numerical modeling and mass balances, *Geochim. Cosmochim. Acta*, *67*(18), 3403–3421.

Luff, R., K. Wallmann, S. Grandel, and M. Schlüter (2000), Numerical modeling of benthic processes in the deep Arabian Sea, *Deep Sea Res., Part II*, *47*, 3039–3072.

Manheim, F. T., and K. M. Chan (1974), Interstitial waters of Black Sea sediments: New data and review, in *The Black Sea—Geology, chemistry and biology*, edited by E. T. Degens and D. A. Ross, *Mem. Am. Assoc. Pet. Geol.*, *20*, 155–180.

Manheim, F. T., and D. M. Schug (1978), Interstitial waters of Black Sea cores, *Initial Rep. Deep Sea Drill. Proj.*, *42*, 637–651.

Martin, J. B., M. Kastner, and H. Elderfield (1991), Lithium: Sources in pore fluids of Peru slope sediments and implications for oceanic fluxes, *Mar. Geol.*, *102*, 281–292.

Martin, J. B., J. M. Gieskes, M. Torres, and M. Kastner (1993), Bromide and iodide in Peru margin sediments and pore fluids: Implications for fluid origins, *Geochim. Cosmochim. Acta*, *57*, 4377–4389.

Martin, J. B., M. Kastner, P. Henry, X. Le Pichon, and S. Lallemant (1996), Chemical and isotopic evidence for sources of fluids in a mud volcano field seaward of the Barbados accretionary wedge, *J. Geophys. Res.*, *101*(B9), 20,325–20,345.

McDuff, R. E., and J. M. Gieskes (1976), Ca and Mg profiles in DSDP drill holes, diffusion or reaction?, *Earth Planet. Sci. Lett.*, *33*, 1–10.

Morozov, N. P. (1969), Geochemistry of the alkali metals in rivers, *Geochem. Int.*, *6*, 585–594.

Müller, P. J., and E. Suess (1979), Productivity, sedimentation rate, and sedimentary organic matter in the oceans—I. Organic carbon preservation, *Deep Sea Res., Part A*, *26*, 1347–1362.

Özsoy, E., and Ü. Ünlüata (1997), Oceanography of the Black Sea: A review of some recent results, *Earth Sci. Rev.*, *42*, 231–272.

Pawellek, F., F. Frauenstein, and J. Veizer (2002), Hydrochemistry and isotope geochemistry of the upper Danube River, *Geochim. Cosmochim. Acta*, *66*(21), 3839–3854.

Pfeifer, K., C. Hensen, M. Adler, F. Wenzhöfer, B. Weber, and H. D. Schultz (2002), Modeling of subsurface calcite dissolution, including the respiration and reoxidation processes of marine sediments in the region of equatorial upwelling off Gabon, *Geochim. Cosmochim. Acta*, *66*(24), 4247–4259.

Pierre, C. (1999), The oxygen and carbon isotope distribution in the Mediterranean water masses, *Mar. Geol.*, *153*, 41–55.

Quinby-Hunt, M. S., and K. K. Turekian (1983), Distribution of elements in seawater, *Eos Trans. AGU*, *64*, 130–131.

Ronov, A. B., A. A. Migdisov, N. T. Voskresenskaya, and G. A. Korzina (1970), Geochemistry of lithium in the sedimentary cycle, *Geochem. Int.*, *7*, 75–102.

Rude, P. D., and R. C. Aller (1994), Fluorine uptake by Amazon continental shelf sediment and its impact on the global fluorine cycle, *Cont. Shelf Res.*, *14*, 883–907.

Sarmiento, J., T. Herbert, and J. Toggweiler (1988), Mediterranean nutrient balance and episodes of anoxia, *Global Biogeochem. Cycles*, *2*, 427–444.

Savin, S. M., and S. Epstein (1970), The oxygen and hydrogen isotope geochemistry of clay minerals, *Geochim. Cosmochim. Acta*, *51*, 1727–1741.

Sayles, F. L. (1979), The composition and diagenesis of interstitial solutions, I: Fluxes across the seawater-sediment interface in the Atlantic Ocean, *Geochim. Cosmochim. Acta*, *43*, 527–545.

Sayles, F. L. (1981), The composition and diagenesis of interstitial solutions, II: Fluxes and diagenesis at the water-sediment interface in the high latitude North and South Atlantic, *Geochim. Cosmochim. Acta*, *45*, 1061–1086.

Seyfried, W. E., D. R. Janecky, and M. J. Mottl (1984), Alteration of the oceanic crust: Implications for geochemical cycles of lithium and boron, *Geochim. Cosmochim. Acta*, *48*, 557–569.

Shimkus, K. M., Y. P. Malovitsky, and S. I. Shumenko (1978), The bedrocks from the Black Sea bottom and some features of the deep-sea basin structure, *Initial Rep. Deep Sea Drill. Proj.*, *42*, 469–482.

Shishkina, O. V. (1978), Distribution of nromine, Cl/Br relationships, and iodine in interstitial water of the Black Sea, based on DSDP Leg 42B, *Initial Rep. Deep Sea Drill. Proj.*, *42*, 631–635.

Smith, H. J., A. J. Spivack, H. Staudigel, and H. Hart (1995), The boron isotope composition of altered oceanic crust, *Chem. Geol.*, *126*, 119–135.

Spivack, A. J., and J. M. Edmond (1987), Boron isotope exchange between seawater and oceanic crust, *Geochim. Cosmochim. Acta*, *51*, 1033–1043.

Spivack, A. J., M. R. Palmer, and J. M. Edmond (1987), The sedimentary cycle of the boron isotopes, *Geochim. Cosmochim. Acta*, *51*, 1939–1949.

Staudigel, H., T. Plank, B. White, and H.-U. Schmincke (1995), Geochemical fluxes during the alteration of the basaltic upper oceanic crust: DSDP Sites 417 and 418, in *Subduction: Top to Bottom*, *Geophys. Monogr. Ser.*, vol. 96, edited by G. E. Bebout et al., pp. 19–38, AGU, Washington, D. C.

Stoffers, P., and G. Müller (1978), Mineralogy and lithofacies of Black Sea sediments Leg 42B Deep Sea Drilling Project, *Initial Rep. Deep Sea Drill. Proj.*, *42*, 373–390.

Stoffyn-Egli, P., and F. T. Mackenzie (1984), Mass balance of dissolved lithium in the ocean, *Geochim. Cosmochim. Acta*, *48*, 859–872.

Stumm, W., and J. J. Morgan (1996), *Aquatic Chemistry*, *Chemical Equilibria and Rates in Natural Waters*, 3rd ed., Wiley-Interscience, New York.

Swart, P. K. (1991), The oxygen and hydrogen isotopic composition of the Black Sea, *Deep Sea Res.*, *38*, Suppl. 2, S761–S772.

Torres, M., H. J. Brumsack, G. Bohrmann, and K. C. Emeis (1996), Barite fronts in continental margin sediments: A new look at barium remobilization in the zone of sulfate reduction and formation of heavy barites in diagenetic fronts, *Chem. Geol.*, *127*, 125–139.

Trimonis, E. S., K. M. Shimkus, P. P. Shirshov, and D. A. Ross (1978), Mineral composition of coarse-silt fraction of the Black Sea Late Cenozoic sediments, *Initial Rep. Deep Sea Drill. Proj.*, *42*, 413–426.

Tryon, M. D., and K. M. Brown (2001), Complex flow patterns through Hydrate Ridge and their impact on seep biota, *Geophys. Res. Lett.*, *28*(14), 2863–2867.

Vengosh, A., Y. Kolodny, A. Starinsky, A. R. Chivas, and M. T. McCulloch (1991), Coprecipitation and isotopic fractionation of boron in modern biogenic carbonates, *Geochim. Cosmochim. Acta*, *55*, 2901–2910.

Wallmann, K. (2001), Controls on the Cretaceous and Cenozoic evolution of seawater composition, atmospheric CO_2 and climate, *Geochim. Cosmochim. Acta*, *65*(18), 3005–3025.

Wallmann, K., P. Linke, E. Suess, G. Bohrmann, H. Sahling, M. Schlüter, A. Dahlmann, S. Lammers, J. Greinert, and N. von Mirbach (1997), Quantifying fluid flow, solute mixing, and biogeochemical turnover at cold vents of the eastern Aleutinan subduction zone, *Geochim. Cosmochim. Acta*, *61*(24), 5209–5219.

Wilson, T. R. S. (1975), Salinity and the major elements of seawater, in *Chemical Oceanography*, vol. 2, edited by J. P. Riley and G. Skirrow, pp. 365–409, Academic, San Diego, Calif.

Woodside, J. M., M. K. Ivanov, and A. F. Limonov (Eds.) (1997), Neotectonics and fluid flow through seafloor sediments in the Eastern Mediterranean and Black Seas, Part II: Black Sea, *IOC Tech. Ser. 48*, 128 pp., UNESCO, Paris.

Yeh, H. W., and S. M. Savin (1977), Mechanism of burial metamorphism of argillaceous sediments: 3. O-isotope evidence, *Geol. Soc. Am. Bull.*, *88*, 1321–1330.

You, C. F., A. J. Spivack, J. H. Smith, and J. M. Gieskes (1993), Mobilization of boron in convergent margins: Implications for the boron geochemical cycle, *Geology*, *21*, 207–210.

You, C. F., A. J. Spivack, J. M. Gieskes, R. Rosenbauer, and J. L. Bishoff (1995), Experimental study of boron geochemistry: Implications for fluid processes in subduction zones, *Geochim. Cosmochim. Acta*, *59*(12), 2435–2442.

You, C. F., P. R. Castillo, J. M. Gieskes, L. H. Chan, and A. J. Spivack (1996), Trace element behavior in hydrothermal experiments: Implications for fluid processes at shallow depths in subduction zones, *Earth Planet. Sci. Lett.*, *140*, 41–52.

Zeebe, R. E., and D. Wolf-Gladrow (2001), *CO_2in Seawater: Equilibrium, Kinetics, Isotopes*, *Elsevier Oceanography Series*, Elsevier Sci., New York.

Zhang, L., L.-H. Chan, and J. M. Gieskes (1998), Lithium isotope geochemistry of pore waters from Ocean Drilling Program Sites 918 and 919, Irminger Basin, *Geochim. Cosmochim. Acta*, *62*(14), 2437–2450.